Neutron diffraction and μSR study on the antiferromagnet $BaCoO_3$

H. Nozaki,[1,*] M. Janoschek,[2,3] B. Roessli,[2] J. Sugiyama,[1] L. Keller,[2] J. H. Brewer,[4] E. J. Ansaldo,[5] G. D. Morris,[5] T. Takami,[6] and H. Ikuta[6]

[1]*Toyota Central Research and Development Laboratories, Inc., Nagakute, Aichi 480-1192, Japan*

[2]*Laboratory for Neutron Scattering, ETH Zurich and Paul Scherrer Institut, CH-5232 Villigen PSI, Switzerland*

[3]*Physik Department E21, TU München, 85748 Garching, Germany*

[4]*TRIUMF, CIAR, and Department of Physics and Astronomy, University of British Columbia, Vancouver, BC V6T 1Z1, Canada*

[5]*TRIUMF, 4004 Wesbrook Mall, Vancouver, BC V6T 2A3, Canada*

[6]*Department of Crystalline Materials Science, Nagoya University, Furo-cho, Chikusa-ku, Nagoya 464-8603, Japan*

(Received 6 June 2006; revised manuscript received 17 October 2006; published 3 July 2007)

The magnetic structure of the antiferromagnetic (AF) hexagonal perovskite $BaCoO_3$ was investigated by neutron diffraction using a powder sample in the temperature range between 60 and 1.5 K. It was found that AF diffraction peaks clearly appear below the Néel temperature (T_N=15 K), which are indexed with the propagation vector $\mathbf{k}=(\frac{1}{3},\frac{1}{3},0)$, indicating that the AF super unit cell is three times larger than the crystallographic unit cell. Data from a parallel muon-spin rotation/relaxation (μ^+SR) measurement allowed the final selection of a unique AF spin structure from several possible spin arrangements compatible with the neutron diffraction pattern. The proposed AF structure is modulated along the (110) direction and described by $\mathbf{m_l}=\mathbf{m}_0\cos(2\pi\mathbf{kl})$, where $\mathbf{m_l}$ is the moment at the Co^{4+} site $\mathbf{l}$ and $\mathbf{m}_0=(0,0,0.53\mu_B)$ at 1.5 K.

DOI: 10.1103/PhysRevB.76.014402 PACS number(s): 76.75.+i, 62.50.+p, 75.30.Kz, 75.25.+z

I. INTRODUCTION

Competition between one-dimensional (1D) and two-dimensional (2D) interactions induces complex physics in the class of hexagonal perovskites ABX_3, in which the face sharing BX_6 octahedra form a 1D BX_3 chain. The chains are located on the corners of the 2D triangular lattice and are separated by A ions.[1] If the 2D interaction is antiferromagnetic (AF), geometrical frustration precludes a typical AF long-range order on the 2D triangular lattice, whether the 1D interaction is AF or ferromagnetic (FM). The hexagonal perovskites are, however, usually classified as a quasi-1D (Q1D) system because the 1D interaction is stronger than the 2D interaction due to the separation between neighboring 1D chains by A ions.

The most established Q1D hexagonal perovskite is, to the authors' knowledge, $CsCoCl_3$, which exhibits successive magnetic transitions from a high-temperature (T) paramagnetic phase to a partially disordered AF (PDA) state at T_{N1} =21 K, and then to a long-range ferrimagnetic phase below T_{N2}=9 K. Strictly speaking, Co^{2+} spins with $S=\frac{1}{2}$ align antiferromagnetically along the $CoCl_3$ chain below T_{N1}, and two-thirds of the neighboring spins in the c plane are also coupled antiferromagnetically, but the remaining one-third remain incoherent in the PDA state ($T_{N2}<T<T_{N1}$). For $T<T_{N2}$, the ferrimagnetically coupled c plane with three sublattices is stacked antiferromagnetically along the c axis.[2] Very similar magnetic structures were also reported for $CsCoBr_3$ below T_{N1}=28 K and T_{N2}=10 K.

The magnetic nature of $CsNiCl_3$ was also thoroughly studied by susceptibility (χ), neutron diffraction (ND), and heat capacity measurements. Two AF transitions were found at 4.85 and 4.4 K,[3,4] but the AF structure was not fully clarified by the ND experiment alone, because there are several possible AF structures compatible with the ND pattern. However, taken together with the results from ^{35}Cl- and ^{133}Cs-NMR experiments, it was determined that one-third of the Ni spins align along the c axis, whereas the remaining two-third lie in the ab plane at T between 4.4 and 4.85 K. Below 4.4 K, the spins in the ab plane rotate by 90° in the plane.

For $BaCoO_3$,[5] it was found that a 1D-FM order appears below 53 K and a sharp bulk 2D-AF transition occurs at 15 K (=T_N) by means of positive muon-spin spectroscopy (μ^+SR) together with heat capacity (C_p) and dc-χ measurements,[6–8] in contrast to the prediction of an electronic structural calculation (local density approximation plus Hubbard u) that a FM ground state is the most stable configuration.[9] Further μ^+SR experiments under pressure up to 1.1 GPa showed that T_N of $BaCoO_3$ is enhanced by pressure, as expected from the relationship between T_N and the interchain distance in the Q1D cobalt oxides.[10] This also strongly supports the role of the 2D-AF interaction on T_N. The zero-field (ZF-) μ^+SR spectrum for $BaCoO_3$ was found to consist of clear but complex oscillations below T_N, with at least five frequency components (ν_μ=14.4, 13.5, 6.4, 5.1, and 3.5 MHz) at 1.8 K under ambient pressure, even though the sample is structurally single phase at room temperature and there is no indication of any structural phase transition down to 4 K.[6] This means that every oxygen is equivalent for the simple hexagonal lattice, as there is naturally only one μ^+ site in the $BaCoO_3$ lattice. In addition, the internal magnetic fields of the five signals, i.e., $\nu_{\mu,i}$, with i=1–5, exhibit a similar T dependence, indicating that the five frequencies are unlikely to be caused by compositional inhomogeneities, but reflect the intrinsic behavior of $BaCoO_3$.

In order to clarify the origin of the multifrequency spectra detected by μ^+SR and to determine the AF structure below T_N, we have carried out neutron powder diffraction (NPD) measurements on $BaCoO_3$ down to 1.5 K. In particular, by combining the NPD results reported here with the μ^+SR data, we conclude that the AF structure is uniquely deter-

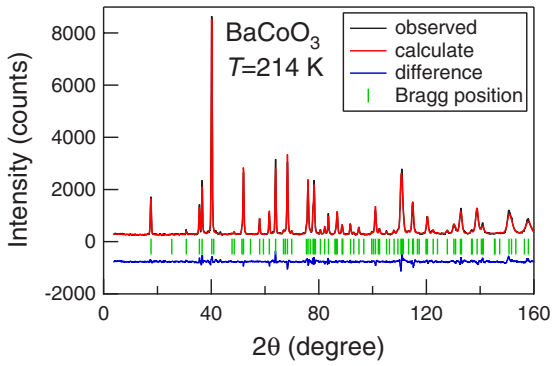

FIG. 1. (Color online) High resolution NPD refinement pattern for $BaCoO_3$ at 214 K.

mined to be not a classical 120° structure but an amplitude modulated structure.

II. EXPERIMENT

A polycrystalline sample of $BaCoO_3$ was synthesized at Nagoya University by a conventional solid state reaction technique using reagent grade Co_3O_4 and $BaCO_3$ powders as starting materials. A sintered pellet was annealed at 650 °C for 150 h in oxygen under 1 MPa pressure, which was subsequently ground in an agate mortar. A powder x-ray diffraction (XRD) analysis showed that the sample was almost single phase $BaCoO_3$ (a_H=0.565 nm, c_H=0.475 nm). The neutron diffraction experiments were performed on the cold neutron powder diffractometer (DMC)[11] and high resolution powder diffractometer for thermal neutrons (HRPT)[12] at the Paul Scherrer Institut (PSI). The wavelength of the neutron beam was 0.2453 nm, monochromatized with pyrolythic graphite (002). The data were analyzed using both FULLPROF (Ref. 13) and RIETAN-2000 (Ref. 14). The μ^+SR experiments were performed on the M20 surface muon beam line at TRIUMF and Dolly at PSI using an experimental setup and techniques that have been described elsewhere.[16]

III. RESULTS

Figure 1 shows the NPD and its Rietveld refinement patterns at 214 K for the $BaCoO_3$ powder measured on HRPT. An analysis of the neutron intensities was carried out with the Rietveld method[17] using the program FULLPROF.[13] The

TABLE I. Results of the Rietveld refinement of neutron powder diffraction data for $BaCoO_3$ at 60 K. Atomic positions for the space group $P6_3/mmc$: Ba at 2*d* $(\frac{1}{3}, \frac{2}{3}, \frac{3}{4})$; Co at 2*a* (0, 0, 0); O at 6*h* $(x, -x, \frac{1}{4})$

		This work	Ref. 18
a (Å)		5.6319(17)	5.65
c (Å)		4.7461(15)	4.749
O	*x*	0.14926(17)	
Agreement factors	χ^2	11.7	
Bragg *R* factor		1.56	

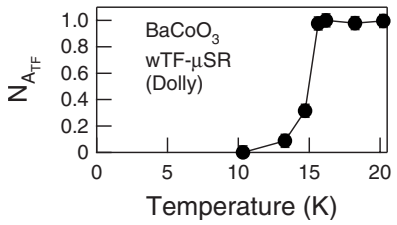

FIG. 2. *T* dependence of the normalized weak transverse field (wTF) asymmetry for the $BaCoO_3$ powder used for the present NPD experiments. The data were obtained by fitting the wTF-μ^+SR spectrum measured at PSI to an exponentially relaxing cosine oscillation signal. A clear magnetic transition is observed at 15 K.

obtained structural parameters are in good agreement with published data,[18] as shown in Table I. The oxygen content is estimated as 2.97±0.05 by the Rietveld refinement, showing that this compound is almost stoichiometric.

The bulk nature of the transition is confirmed by the data in Fig. 2, which shows the *T* dependence of the normalized weak transverse field (wTF) asymmetry ($N_{A_{TF}}$) for the $BaCoO_3$ sample used in the NPD experiments. Since $N_{A_{TF}}$, estimated from the wTF-μ^+SR data (here, wTF=50 Oe), is proportional to the volume fraction of paramagnetic phases,[16] the $N_{A_{TF}}(T)$ curve therefore shows that the whole sample enters into the magnetic phase below ~15 K, while it is fully paramagnetic above 15 K.

Figure 3 shows the DMC diffraction patterns obtained at (a) 60 K and (b) 1.5 K—i.e., well above and below T_N. The additional (weak) peaks below T_N are ascribed to the AF order of the Co spins. In order to display the additional three peaks more clearly, Fig. 4 shows the difference between the

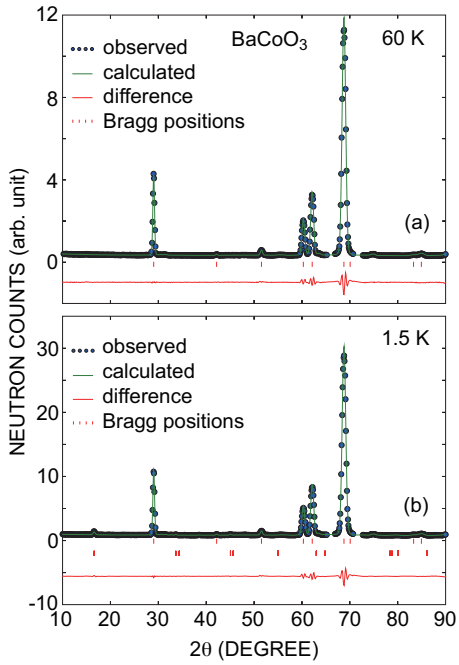

FIG. 3. (Color online) Refinements of the powder diffraction patterns for $BaCoO_3$ at (a) T=60 K and (b) 1.5 K. The two excluded regions at $2\theta \sim 66°$ and 72° are due to an undetermined impurity in the powder sample.

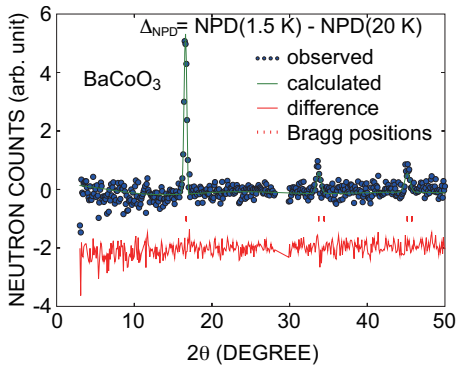

FIG. 4. (Color online) Refinement of the difference diffraction pattern (Δ_{NPD}) for $BaCoO_3$. The Δ_{NPD} pattern was produced by subtracting the $T=20$ K data set from the data collected at $T=1.5$ K. Scattering angles where strong nuclear reflections are present were excluded from the graph. Only the data points for scattering angles up to 50° were included in the analysis. As for larger angles, magnetic intensities are not observed due to their magnetic form factor.

spectra obtained at 1.5 K and at 20 K (Δ_{NPD}). Note that no extra intensity is observed in the nuclear reflections at both T's. The difference spectrum Δ_{NPD} is thus assigned to the magnetic structure. In addition, Fig. 5 shows the T dependence of the NPD pattern in three dimensions to fully display the whole T range measured.

The magnetic Bragg reflections are indexed with a propagation vector $\mathbf{k}=(\frac{1}{3},\frac{1}{3},0)$—that is, the magnetic unit cell is three times larger than the chemical one. Four possible models, in agreement with the crystal symmetry and the propagation vector $\mathbf{k}$, were identified by a representational analysis as described in the Appendix. Figure 6 shows the four magnetic structures. Here, Γ_3 corresponds to an amplitude modulated (am) structure with moments aligned ferromagnetically along the crystallographic c direction propagating in the (1, 1, 0) direction with a period of 3**a** [see Fig. 6(a)]. Γ_5 describes a magnetic structure where the spins along the Co chains have a FM arrangement and form a 120° configuration in the hexagonal plane, i.e., a 120° structure [see Fig. 6(c)]. The other two representations Γ_4 and Γ_6 correspond to models similar to Γ_3 and Γ_5, respectively, but for which the coupling along the c directions is AF [see Figs. 6(b) and 6(d)].

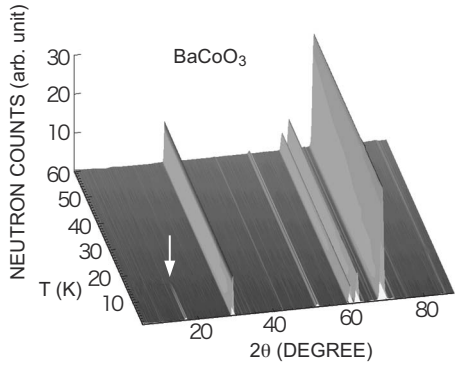

FIG. 5. Evolution of the NPD patterns of $BaCoO_3$ from $T=1.5$ to 60 K. At around 15 K, an additional reflection appears (arrow) due to the onset of the AF order. There are two more magnetic reflections which can only be seen clearly in a difference plot (see Fig. 4) because of their very weak intensities. Above 15 K, the patterns are identical.

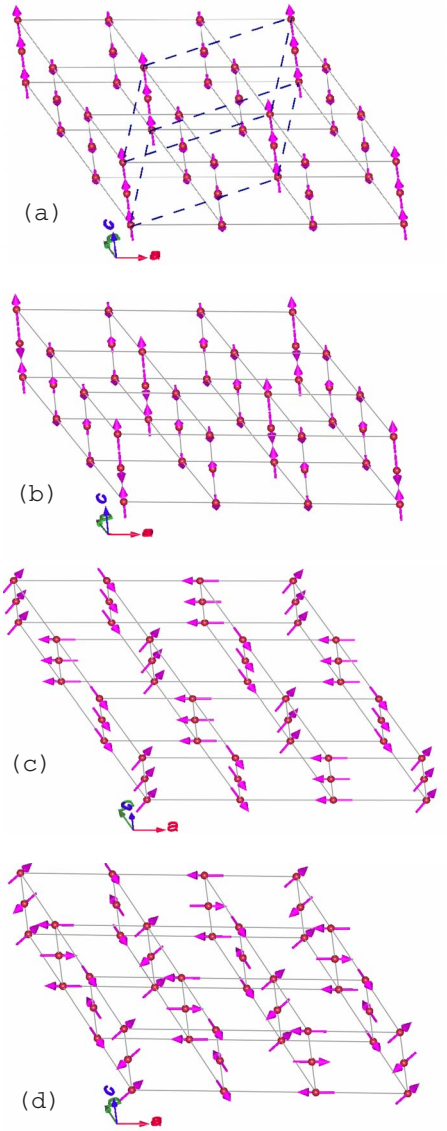

FIG. 6. (Color online) Magnetic structures corresponding to the four possible irreducible representations. Because the propagation vector is $\mathbf{k}=(\frac{1}{3},\frac{1}{3},0)$, the magnetic unit cell is three times larger than the nuclear one, as shown in (a). The lattice constants of the magnetic unit are $a'=\sqrt{3}\times a$ and $c'=c$. Only the Co atoms in the layers with $z=0$ and $z=0.5$ are shown. (a) Γ_3, (b) Γ_4, (c) Γ_5, and (d) Γ_6. The figures were generated with the program FULLPROF STUDIO (Ref. 13).

A least-squares fit of the Δ_{NPD} pattern suggests that both representations Γ_3 or Γ_5 are suitable solutions for the AF structure since their magnetic R factors $R_M=6.47$ for Γ_3 and $R_M=6.48$ for Γ_5 are very similar. The other two possible models yield significantly worse agreement factors ($R_M>60$) and are hence inadequate. We note that the nature of the magnetic order is purely three dimensional in $BaCoO_3$.

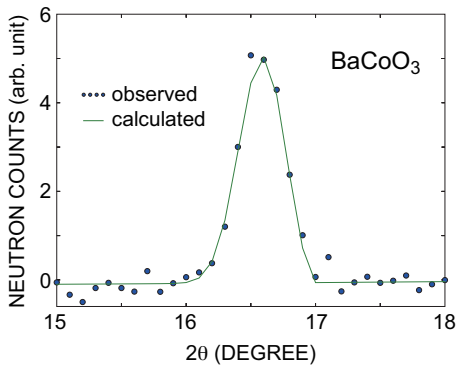

FIG. 7. (Color online) Magnified magnetic Bragg peak for $BaCoO_3$ at $2\theta=16.5°$. The symmetrical peak shape suggests the 3D nature of the AF order.

This is because a 2D magnetic order is known to lead to rods of magnetic intensity in reciprocal space, and the magnetic neutron profile of the magnetic reflections becomes asymmetric,[15] which is not the case for our data (see Fig. 7). Also, the T dependence of the ordered magnetic moment is very similar to that of the internal magnetic field detected by μ^+SR (see Fig. 8), for which the critical exponent $\beta=0.191\pm0.009$ (Ref. 6) lies between the predictions for the 2D and three-dimensional (3D) Ising model ($\beta=0.125$ and 0.3125).

The magnetic moments (m_0), determined at the lowest T measured, were $0.53(2)\mu_B$ for Γ_3 and $0.51(6)\mu_B$ for Γ_5, identical within experimental errors. Hence, it is found that the ordered moment is significantly reduced from the expected value $m_0=1\mu_B$ for Co^{4+} ions in the low-spin state with $S=1/2$. Although the origin of such reduction is still unknown, partially due to a lack of information on exchange interactions, we propose the following two scenarios. On one hand, considering $BaCoO_3$ as a Q1D system, the reduction would be a consequence of a weak coupling between the Co chains, $(J_\perp/J)\ll 1$, where $J_\perp$ and J are the magnetic inter- and intrachain coupling constants, respectively.[19–21] On the other hand, if we assume that $BaCoO_3$ is a representative of a stacked triangular antiferromagnet, the reduction is naturally induced by a geometric frustration in the hexagonal plane.[22]

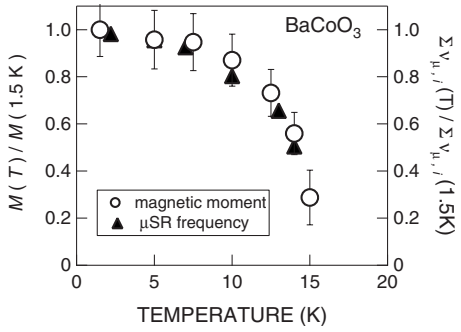

FIG. 8. Temperature dependence of the ordered magnetic moment for $BaCoO_3$, estimated from the strongest magnetic Bragg peak at $\frac{1}{3}\frac{1}{3}0$, observed around $2\theta=16.7°$. The magnetic moment is shown normalized to the moment at 1.5 K [$N_M=M(T)/M(1.5\text{ K})$]. The right vertical axis shows the average of the normalized muon-spin precession frequencies obtained by ZF-μ^+SR (Ref. 6).

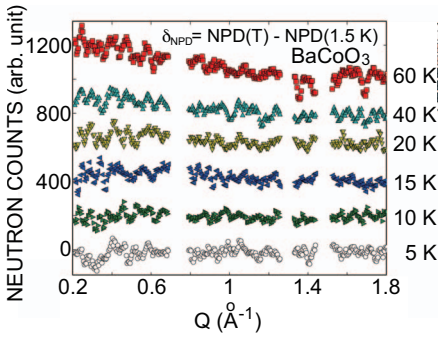

FIG. 9. (Color online) Temperature dependence of the diffuse paramagnetic scattering for $BaCoO_3$ obtained by subtracting the NPD pattern at 1.5 K from that at each T point [$\delta_{\rm NPD}(T)$ =NPD(T)-NPD(1.5 K)]. Bragg peaks were removed from the data and the data were smoothed within a width of 0.01 Å^{-1}. Each $\delta_{\rm NPD}(T)$ curve is offset by 200 for clarity of display.

The existence of FM clusters with diameters of approximately 1.2 nm and separated by an average distance of about 3 nm was proposed for $BaCoO_3$ (Refs. 7 and 23) from the analysis of magnetization data, which indicated a blocking temperature of $T_B=50$ K for the clusters, where the slope of the magnetization curve changes. Above T_B, $BaCoO_3$ exhibits superparamagnetism, which would also be consistent with the cluster model, and the $\chi(T)$ curve follows the Curie law only for T above 250 K. Our χ measurement also suggests the existence of weak FM or ferrimagnetic order above T_N with an ordering temperature $T_C=53$ K. In the wTF μ^+SR experiment, as T decreases from 100 K, the relaxation rate ($\lambda_{\rm TF}$) is almost T independent down to T_C, then increases slightly, and finally increases very rapidly below T_N. The wTF asymmetry, shown in ($A_{\rm TF}$) is T independent and close to the maximum possible value (~0.23 in our setup) above T_N (see Fig. 2), suggesting the absence of a quasistatic magnetic order above T_N. This result does not, however, preclude the existence of nanometer-scale FM clusters for several reasons. The relatively small volume fraction, i.e., the fraction of muons stopping inside clusters, can be roughly estimated to be less than $0.064=(1.2/3)^3$. Their (weak) internal fields, inhomogeneous and fluctuating enough that the muon spins inside clusters, are not depolarized, but still affect the empirical $\lambda_{\rm TF}$ slightly. In other words, the wTF experiments are not sensitive enough for this situation.

In order to elucidate the appearance of the paramagnetic signal in the NDP data, Fig. 9 shows the $\delta_{\rm NPD}$ spectra from 5 to 60 K, where $\delta_{\rm NPD}(T)=\text{NPD}(T)-\text{NPD}(1.5\text{ K})$. The paramagnetic contribution to the neutron cross section is given by

$$\frac{d\sigma}{d\Omega}\propto F^2(\vec{Q})S(S+1), \tag{1}$$

where $F(\vec{Q})$ is the magnetic form factor. A T-independent diffuse scattering in the neutron diffraction pattern should be therefore observed above T_N. Nevertheless, as shown in Fig.

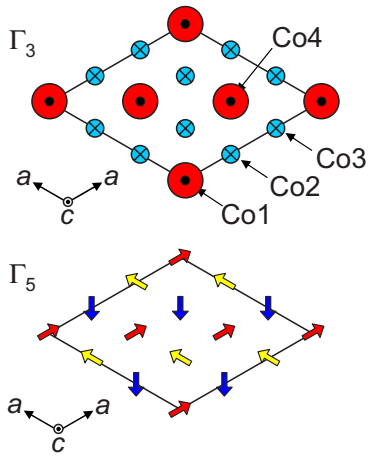

FIG. 10. (Color online) Γ_3: Co moments align along the c axis with an amplitude modulation. The magnitude of the Co moments antiparallel to the c axis is half of that parallel to the c axis. Γ_5: Classical AF 120° structure. The angle between two adjacent Co moments is 120°, and the sum of the three Co moments, which are located at the corners of the triangle, is zero.

9, the δ_{NPD} spectrum does not clearly reveal the presence of the expected paramagnetic scattering immediately above T_N. Only at $T > \sim 40$ K, a diffuse scattering is obviously observed at low scattering angles. In addition, the scattering intensity increases with T up to at least 60 K. Such variation in the diffuse scattering with T is a signature for the existence of short-range correlations in $BaCoO_3$ even above T_N. As T increases further from 40 K, since the diffuse scattering grows with T, the correlation length naturally decreases (and eventually disappears) until a paramagnetic regime is really suitable for $BaCoO_3$. The neutron diffraction data are hence consistent with the results of dc-χ and μ^+SR; that is, a FM behavior below T_C=53 K and the absence of a long-range order above T_N. In other words, the present combination of NPD and μ^+SR experiments just indicates that the ordering below T_C=53 K is short ranged and fast fluctuating.

IV. DISCUSSION

Among several possible structures that would explain the magnetic super unit cell, good fits were obtained with both Γ_3 and Γ_5 (see Fig. 10). The former is an amplitude modulated structure, in which two distinct Co ions form a modulated structure, while the latter is a classical 120° AF structure. Since $R_M(\Gamma_3) \approx R_M(\Gamma_5)$, however, the neutron data alone cannot discriminate between the two models.

The ZF-μ^+SR experiment showed two dominant internal fields, ($H_{\mathrm{int},H}$ and $H_{\mathrm{int},L}$, with $H_{\mathrm{int},H} > H_{\mathrm{int},L}$) below T_N (see Fig. 11), in spite of the fact that μ^+ sites must be crystallographically equivalent even at 1.8 K (Ref. 6) (the μ^+ is located in the vicinity of the CoO_3 chain[10]). This indicates that the Γ_3 structure is most likely to be the magnetic structure of $BaCoO_3$ because the μ^+ would experience only one internal field in the classical 120° AF structure. A dipole field calculation, in which we consider the effect of the nearest seven CoO_3 chains within the nearest four Co planes, yields local

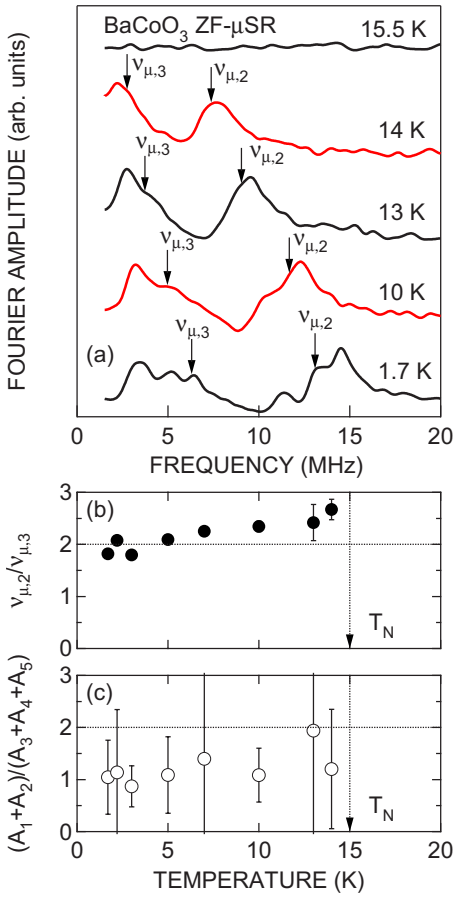

FIG. 11. (Color online) (a) Fourier transform of the ZF-μ^+SR spectrum for $BaCoO_3$ obtained at TRIUMF. The two wide maxima below T_N=15 K show the existence of two different internal fields in $BaCoO_3$, although all the possible μ^+ sites are crystallographically equivalent in the lattice. (b) The ratio of the two precession frequencies ($\nu_{\mu,2}$ and $\nu_{\mu,3}$) as a function of T. Each is the mean frequency for the corresponding broad maximum. Since the ZF-μ^+SR spectra were fitted with five oscillating signals $\Sigma A_i \cos(\nu_{\mu,i} \times 2\pi t + \phi)$ (i=1–5) (Ref. 6), (c) shows the ratio between the amplitudes of the higher frequency signals (A_1 and A_2) and the lower frequency signals (A_3, A_4, and A_5). The broken lines in (b) and (c) show the prediction from the dipole field calculation.

magnetic fields at the μ^+ site of 1620 and 810 Oe if $\mathbf{m}_0 = (0,0,1\mu_B)$ in the Γ_3 structure. From the observed precession frequencies of the two main signals, $\nu_{\mu,2}$=13.1 MHz (H=989 Oe) and $\nu_{\mu,3}$=6.30 MHz (H=466 Oe), $\mathbf{m}_0$ is estimated to be $(0,0,0.61\mu_B)$ at 1.7 K, which is in good agreement with the value obtained from the NPD measurement [$(0,0,0.53\mu_B)$ at 1.5 K]. The ratio $\nu_{\mu,H}$ and $\nu_{\mu,L}$=2.08 is very close to the prediction of the dipole field calculation ($\nu_{\mu,H}/\nu_{\mu,L}$=2) over the whole range of measured temperatures [see Fig. 11(b)]. These facts strongly suggest that Γ_3 is the most reasonable structure for $BaCoO_3$ in the T range between 1.5 and 15 K. Figures 11(b) and 11(c) also show that the magnetic structure does not change down to 1.5 K in contrast to $CsNiCl_3$.[3,4]

The classical 120° AF is a common structure for the AF 2D triangular lattice with half-filling. Furthermore, several hexagonal ABX_3-type double halides do not have an axial

TABLE II. Irreducible representations for the space group $P6_3/mmc$ with the propagation vector $\mathbf{k}=(\frac{1}{3},\frac{1}{3},0)$. $\omega=\exp(2\pi i/3)$.

v	1	$3^+_{0,0,z}$	$3^-_{0,0,z}$	$2_{x,x,0}$	$2_{x,0,0}$	$2_{0,y,0}$	$m(x,y,1/4)$	$6^-_{0,0,z}$	$6^+_{0,0,z}$	$c(x,x,z)$	$c(x,0,z)$	$c(0,y,z)$
Γ_1	1	1	1	1	1	1	1	1	1	1	1	1
Γ_2	1	1	1	1	1	1	−1	−1	−1	−1	−1	−1
Γ_3	1	1	1	−1	−1	−1	1	1	1	−1	−1	−1
Γ_4	1	1	1	−1	−1	−1	−1	−1	−1	1	1	1
Γ_5	I^a	$B_1{}^b$	$B_2{}^c$	A^d	$B_3{}^e$	$B_4{}^f$	$-I$	$-B_1$	$-B_2$	$-A$	$-B_3$	$-B_4$
Γ_6	I^a	$B_1{}^b$	$B_2{}^c$	A^d	$B_3{}^e$	$B_4{}^f$	I	$B_1{}^b$	$B_2{}^c$	A^d	$B_3{}^e$	$B_3{}^e$

[a] $I=\begin{pmatrix}1&0\\0&1\end{pmatrix}$.
[b] $B_1=\begin{pmatrix}\omega&0\\0&\omega^*\end{pmatrix}$.
[c] $B_2=\begin{pmatrix}\omega^*&0\\0&\omega\end{pmatrix}$.
[d] $A=\begin{pmatrix}0&1\\1&0\end{pmatrix}$.
[e] $B_3=\begin{pmatrix}0&\omega^*\\\omega&0\end{pmatrix}$.
[f] $B_4=\begin{pmatrix}0&\omega\\\omega^*&0\end{pmatrix}$.

magnetic structure, but rather a spin spiral structure.[24,25] It was, however, found that the Γ_3 structure appears below T_N for $BaCoO_3$, given by $\mathbf{m_l}=\mathbf{m}_0\cos(2\pi\mathbf{kl})$, where $\mathbf{m_l}$ is the moment at the Co^{4+} site $\mathbf{l}$, $m_0=(0,0,0.53\mu_B)$ at 1.5 K, and $\mathbf{k}$ is the propagation vector $(\frac{1}{3},\frac{1}{3},0)$.

V. CONCLUSION

In order to clarify the origin of the five components detected by μ^+SR and to determine the magnetic structure below T_N, we have performed a NPD experiment on $BaCoO_3$ down to 1.5 K. We found clear magnetic diffraction peaks below T_N, indicating the appearance of a new three-sublattice AF structure. Since the muons experience mainly two different fields in spite of the single crystallographic μ^+ site in the lattice, we concluded that the spin structure is not a classical 120° AF domain structure but the Γ_3 structure represented by $\mathbf{m_l}=\mathbf{m}_0\cos(2\pi\mathbf{kl})$, where $\mathbf{m_l}$ is the moment at the Co^{4+} site $\mathbf{l}$, $m_0=(0,0,0.53\mu_B)$ at 1.5 K, and $\mathbf{k}$ is the propagation vector $(\frac{1}{3},\frac{1}{3},0)$. The NPD refinements could not, by themselves, distinguish between a classical 120° AF domain structure and a Γ_3 structure.

Since $BaCoO_3$ is an insulator even at ambient temperature, the Γ_3 structure naturally leads to a periodic modulation on the Co ions—i.e., a charge density wave (CDW) state. However, the CDW modulation is thought to be too small for detection by XRD or electron diffraction because the variation of charge is simply estimated to be about $\pm\frac{1}{2}$ for $m_0=0.53\mu_B$. Although the origin of the Γ_3 structure is still not fully understood, the 1D nature probably plays a significant role in its appearance. As previously reported, the 1D-FM order along the CoO_3 chain is complete below $T_C=53$ K for $BaCoO_3$, each chain acting as a single spin so as to form the 2D-AF order detected by both μ^+SR and NPD. This means that the spin direction is strongly restricted to be either parallel or antiparallel along the chain, i.e., a typical Ising AF. For this reason, the classical 120° structure is unlikely to be stable in $BaCoO_3$, although the structure is more favorable for minimizing electrostatic repulsion due to a homogeneous charge distribution. To further elucidate the origin of the amplitude modulated AF (Γ_3) structure for $BaCoO_3$, experiments using single crystals are necessary, as well as an accurate electrostructural calculation.

ACKNOWLEDGMENTS

The neutron work was performed at the Paul Scherrer Institut, and the μ^+SR work at both TRIUMF and PSI. The authors thank the SINQ staff of PSI for help with the neutron scattering experiments, and the μSR facility staff of TRIUMF and the LMU staff of PSI for help with the μ^+SR experiments. They also appreciate Y. Ikedo of Toyota CRDL, and A. Amato and D. Andreica of PSI for helpful discussion. Further, they thank V. Pomjakushin of PSI for HRPT data and advice with the representational analysis. T.T. acknowledges gratefully the support of JSPS Research Foundation for Young Scientists. H.N. and J.S. are partially supported by the KEK-MSL Inter-University Program for Overseas Muon Facilities. This work is also supported by Grant-in-Aid for Scientific Research (B) (19340107) 2007–2009.

TABLE III. Basis vectors for the magnetic modes on the Co site (2*a*). Here, $\epsilon=\sqrt{3}$.

IR	Co1 (0,0,0)	Co2 (0,0,0.5)
Γ_3	(0,0,1)	(0,0,1)
Γ_4	(0,0,1)	(0,0,−1)
Γ_5	$\left(1-\frac{i}{\epsilon},-\frac{2i}{\epsilon},0\right)$	$\left(1-\frac{i}{\epsilon},-\frac{2i}{\epsilon},0\right)$
	$\left(\frac{2i}{\epsilon},1+\frac{i}{\epsilon},0\right)$	$\left(\frac{2i}{\epsilon},1+\frac{i}{\epsilon},0\right)$
Γ_6	$\left(1-\frac{i}{\epsilon},-\frac{2i}{\epsilon},0\right)$	$\left(-1+\frac{i}{\epsilon},+\frac{2i}{\epsilon},0\right)$
	$\left(\frac{2i}{\epsilon},1+\frac{i}{\epsilon},0\right)$	$\left(-\frac{2i}{\epsilon},-1-\frac{i}{\epsilon},0\right)$

APPENDIX: IRREDUCIBLE REPRESENTATIONS FOR THE MAGNETIC STRUCTURE

The possible magnetic structures in agreement with the crystal symmetry can be found by means of a representational analysis according to Bertaut.[26] The programs BASIREPS (Ref. 13) and MODY (Ref. 27) were used to perform this analysis for the space group $P6_3/mmc$. For the propagation vector $\mathbf{k}=(\frac{1}{3},\frac{1}{3},0)$, the irreducible representations of the little group $G_{\mathbf{k}}$ are Γ_i $(i=1-6)$ given in Table II. Representations 1–4 are unidimensional, whereas 5 and 6 are two dimensional.

The decomposition of Γ in terms of the irreducible representations of $G_{\mathbf{k}}$ is found to be

$$\Gamma = \Gamma_3 + \Gamma_4 + \Gamma_5 + \Gamma_6. \tag{A1}$$

Therefore, the representations Γ_1 and Γ_2 do not contribute to the little group. The basis vectors of the representations 3–6 are given in Table III. In Γ_3 the moments on the Co sites are aligned along the crystallographic c direction and are coupled ferromagnetically between the layers $z=0$ and $z=0.5$. Due to the propagation vector $\mathbf{k}=(\frac{1}{3},\frac{1}{3},0)$, the magnetic structure corresponds to an amplitude modulated structure with a period of three unit cells, where the magnetic moments are parallel to the c direction. Γ_4 also corresponds to such an amplitude modulated structure along the c direction, with the difference that the magnetic moments between the layers $z=0$ and $z=0.5$ are coupled antiferromagnetically. For Γ_5 and Γ_6 the magnetic moments are confined in the hexagonal ab plane. Inside one plane, the moments form a 120° structure and are coupled ferromagnetically and antiferromagnetically between the $z=0$ and $z=0.5$ planes for the Γ_5 and Γ_6 representations, respectively. The bidimensionality of the two representations allows for a free rotation of the moments inside the ab plane, with the constraint that their mutual orientation is kept in accordance with a 120° structure. The structures belonging to each of the four possible representations are shown in Fig. 6.

*e1236@mosk.tytlabs.co.jp

[1] T. Li, G. D. Stucky, and G. L. McPherson, Acta Crystallogr., Sect. B: Struct. Crystallogr. Cryst. Chem. **29**, 1330 (1973).
[2] N. Achiwa, J. Phys. Soc. Jpn. **27**, 561 (1969).
[3] R. H. Clark and W. G. Moulton, Phys. Rev. B **5**, 788 (1972).
[4] W. B. Yelon and D. E. Cox, Phys. Rev. B **7**, 2024 (1973).
[5] Y. Takeda, J. Solid State Chem. **15**, 40 (1975).
[6] J. Sugiyama, H. Nozaki, J. H. Brewer, E. J. Ansaldo, T. Takami, H. Ikuta, and U. Mizutani, Phys. Rev. B **72**, 064418 (2005).
[7] K. Yamaura, H. W. Zandbergen, K. Abe, and R. J. Cava, J. Solid State Chem. **146**, 96 (1999).
[8] K. Yamaura and R. J. Cava, Solid State Commun. **115**, 301 (2000).
[9] V. Pardo, P. Blaha, M. Iglesias, K. Schwarz, D. Baldomir, and J. E. Arias, Phys. Rev. B **70**, 144422 (2004).
[10] J. Sugiyama, H. Nozaki, Y. Ikedo, K. Mukai, D. Andreica, A. Amato, J. H. Brewer, E. J. Ansaldo, G. D. Morris, T. Takami, and H. Ikuta, Phys. Rev. Lett. **96**, 197206 (2006).
[11] P. Fischer and L. Keller, Neutron News **11**, 19 (2000).
[12] P. Fischer, G. Frey, M. Koch, M. Könnecke, V. Pomjakushin, J. Schefer, R. Thut, N. Schlumpf, R. Bürge, U. Greuter, S. Bondt, and E. Berruyer, Physica B **276–278**, 146 (2000).
[13] J. Rodriguez-Carvajal, Physica B **192**, 55 (1993).
[14] F. Izumi and T. Ikeda, Mater. Sci. Forum **321–324**, 198 (2000).
[15] B. Roessli, P. Fischer, U. Staub *et al.*, Europhys. Lett. **23**, 511 (1993).
[16] G. M. Kalvius, D. R. Noakes, and O. Hartmann, in *Handbook on the Physics and Chemistry of Rare Earths*, edited by K. A. Gschneidner, Jr. *et al.* (North-Holland, Amsterdam, 2001), Vol. 32, pp. 51–55, and references cited therein.
[17] H. M. Rietveld, J. Appl. Crystallogr. **2**, 65 (1969).
[18] H. Taguchi, Y. Takeda, F. Kanamaru, M. Shimada, and M. Koizumi, Acta Crystallogr., Sect. B: Struct. Crystallogr. Cryst. Chem. **33**, 1298 (1977).
[19] H. J. Schulz, Phys. Rev. Lett. **77**, 2790 (1996).
[20] K. M. Kojima, Y. Fudamoto, M. Larkin, G. M. Luke, J. Merrin, B. Nachumi, Y. J. Uemura, N. Motoyama, H. Eisaki, S. Uchida, K. Yamada, Y. Endoh, S. Hosoya, B. J. Sternlieb, and G. Shirane, Phys. Rev. Lett. **78**, 1787 (1997).
[21] I. A. Zaliznyak, C. Broholm, M. Kibune, M. Nohara, and H. Takagi, Phys. Rev. Lett. **83**, 5370 (1999).
[22] T. J. Sato, S.-H. Lee, T. Katsufuji, M. Masaki, S. Park, J. R. D. Copley, and H. Takagi, Phys. Rev. B **68**, 014432 (2003).
[23] V. Pardo, J. Rivas, D. Baldomir, M. Iglesias, P. Blaha, K. Schwarz, and J. E. Arias, Phys. Rev. B **70**, 212404 (2004).
[24] M. Melamud, H. Pinto, J. Makovsky, and H. Shaked, Phys. Status Solidi B **63**, 699 (1974).
[25] V. J. Minkiewicz, D. E. Cox, and G. Shirane, J. Phys. (Paris), Colloq. **32**, C1–892 (1971).
[26] E. F. Bertaut, *Magnetism*, edited by G. T. Rado and H. Shul (Academic, New York, 1963), Vol. III, Chap. 4, p. 149.
[27] W. Sikora, F. Bialas, and L. Pytlik, J. Appl. Crystallogr. **37**, 1015 (2004).